MR imaging features of pancreatic acinar cell carcinoma

D. Jornet, P. Soyer, B. Terris, C. Hoeffel, A. Oudjit, P. Legmann, S. Gaujoux, M. Barret, A. Dohan

MR imaging features of pancreatic acinar cell carcinoma

Diane Jornet, MD[1] , Philippe Soyer, MD, PhD[1,2,3] , Benoit Terris, MD, PhD[2,4] , Christine Hoeffel, MD, PhD[5] , Ammar Oudjit, MD[1] , Paul Legmann, MD[1] , Sébastien Gaujoux MD, PhD[2,6], Maximilien Barret, MD, PhD[2,7] , Anthony Dohan, MD, PhD[1,2,3*]

[1]Department of Abdominal & Interventional Radiology, Hôpital Cochin, AP-HP, 27 Rue du Faubourg Saint-Jacques, 75014 Paris, France

[2]Université Descartes Paris 5, Sorbonne Paris Cité, rue de l'Ecole de Médecine, 75006 Paris, France

[3]UMR INSERM 965, 2 rue Amboise Paré, 75010 Paris, France

[4]Department of Pathology, Hôpital Cochin, AP-HP, 27 Rue du Faubourg Saint-Jacques, 75014 Paris, France

[5]Department of Radiology, Hôpital Robert Debré, 11 Boulevard Pasteur, 51092 Reims, France

[6]Department of Abdominal Surgery, Hôpital Cochin, AP-HP, 27 Rue du Faubourg Saint-Jacques, 75014 Paris, France

[7]Department of Gastroenterology, Hôpital Cochin, AP-HP, 27 Rue du Faubourg Saint-Jacques, 75014 Paris, France

***Corresponding author**: anthony.dohan@aphp.fr

The authors have no conflicts of interest to disclose regarding this manuscript.

This study did not receive specific funding.

Abstract

Purpose: This study aimed to report the magnetic resonance imaging (MRI) features of acinar cell carcinoma (ACC) of the pancreas including diffusion-weighted MRI findings.

Material and method: The MRI examinations of five patients (3 men, 2 women; median age, 61 years) with histopathologically proven ACC of the pancreas were retrospectively reviewed. MR images were analyzed qualitatively (location, shape, homogeneity, signal intensity, vascular involvement and extrapancreatic extent of ACC) and quantitatively (tumor size, apparent diffusion coefficient [ADC] and normalized ADC of ACC).

Results: All ACC were visible on MRI, presenting as an oval pancreatic mass (5/5; 100%), with moderate and heterogeneous enhancement (5/5; 100%), with a median transverse diameter of 43 mm (Q_1, 35; Q_3, 82 mm; range: 30 – 91 mm). Tumor capsule was visible in 4/5 ACC (80%) and Wirsung duct enlargement in 2/5 ACC (40%). On diffusion-weighted MRI, all ACC (5/5; 100%) were hyperintense on the 3 b value images. Median ADC value of ACC was 1.061×10^{-3} mm^2/sec (Q_1, 0.870×10^{-3} mm^2/sec; Q_3, 1.138×10^{-3} mm^2/sec; range: 0.834-1.195 $\times 10^{-3}$ mm^2/sec). Median normalized ADC ratio of ACC was 1.127 (Q_1, 1.071; Q_3, 1.237; range: 1.054-1.244).

Conclusions: On MRI, ACC of the pancreas presents as a large, oval pancreatic mass with moderate and heterogeneous enhancement after intravenous administration of a gadolinium chelate, with restricted diffusion and a median ADC value of 1.061 x 10^{-3} mm^2/sec on diffusion-weighted MRI. Further studies however are needed to confirm our findings obtained in a limited number of patients.

Index terms: MR imaging (MRI); Acinar cell carcinoma of the pancreas; Diffusion-weighted MR imaging; Pancreatic neoplasms; Tissue characterization

Introduction

Most of pancreatic tumors are adenocarcinomas [1]. However, the pancreas can be involved by myriad other tumors so that one role of imaging is lesion characterization [2-7]. Computed tomography (CT) is still considered as the standard of reference for the diagnosis of pancreatic tumors [1]. However, magnetic resonance imaging (MRI), including diffusion-weighted sequences, is now emerging as a problem solving tool in patients with pancreatic tumor because of high capabilities for tumor characterization by comparison with CT [8-11].

Acinar cell carcinoma (ACC) of the pancreas accounts for less than 1% of pancreatic neoplasms [12]. This tumor originates from acinar elements of the exocrine pancreas [12, 13]. The diagnosis of ACC of the pancreas is usually not straightforward because patients with this condition may present with nonspecific symptoms similar to those of the more common ductal adenocarcinoma [13]. In addition histopathological diagnosis may be challenging using fine-needle aspiration biopsy [14, 15]. Finally, specific histochemical stainings are required for a definite diagnosis but they are not routinely performed [15]. As a consequence imaging plays a pivotal role to suggest the diagnosis of ACC and alert the clinician and the pathologist should this diagnosis be within the range of plausible ones. This role is rendered more critical because ACC conveys a better prognosis than the more common ductal adenocarcinoma [12, 13].

The computed tomography (CT) features of ACC have been reported in several studies and some suggestive features have been identified [6, 15-21]. However, ACC of the pancreas may sometimes display nonspecific or misleading features on CT (14, 17, 22-24]. As a consequence, it may be reasonably assumed that MRI, owing to better degrees of tissue characterization by comparison with CT, may help improve the degree of confidence with which ACC can be characterized. The MRI findings of ACC of the pancreas have received little attention in the literature to date [25-28]. In addition, their presentation on diffusion-weighted (DW) MRI has not been reported yet.

The purpose of this study was to report the MRI presentation of ACC of the pancreas including DW-MRI findings.

Materials and methods

Patients

The databases of the departments of pathology, surgery and gastroenterology of our institutions were queried from January 2012 to December 2017. The initial search retrieved a total of 20 patients with pancreatic ACC. A cross match was performed with the database of the departments of radiology to identify those who had had MRI examination in our institution.

The study population consisted of five patients (3 men, 2 women) with ACC of the pancreas with a median age of 61 years (Q1, 49; Q3, 77; range: 38-87 years) who had MRI examination available for review. For the five patients, the final diagnosis of ACC of the

pancreas was obtained after histopathological analysis of biopsy specimens (n = 1) or resected specimens (n=4) obtained after distal pancreatectomy (n=3) or duodenopancreatectomy (n=1). This non-interventional, retrospective analysis of data was approved by our review boards and informed consent was waived.

MRI

MRI examinations were performed using a 1.5 T unit (Avanto® or Aera®, Siemens Healthineers). The MR pulse sequences included axial fat suppressed T2-weighted fast spin echo (TR/TE = 2700-3500/70-92 msec; echo train length [ETL] = 17; field of view [FOV] = 320-380; matrix size = 288 × 384), axial T2-weighted HASTE (TR/TE = 1,000-11,000/80-91 msec; ETL = 256; FOV = 320-380 mm; matrix size = 256 × 256), axial diffusion-weighted (DW) (TR/TE = 5,280-7,000/58-83 msec; matrix size, 182 × 192; FOV = 320-380 mm; b values = 50, 400-500, 800-1000 s/mm^2) and fat-suppressed axial T1-weighted three-dimensional volumetric interpolated breath-hold (3D VIBE) gradient-echo (TR/TE = 3.1-5.6 msec/1.6-2.8 msec; flip angle = 10-15°; matrix size = 240-340 × 320-400) MR images before and 30, 60, 90 seconds and 3 minutes after intravenous administration of 0.2 mL/kg of a gadolinium-based contrast agent (Gadoterate meglumine, Dotarem®, Laboratoire Guerbet) [29]. All patients had MR cholangiopancreatography (MRCP) using two-dimensional and 3D sequences.

Image analysis

Anonymized MRI examinations were analyzed by two observers working in consensus using a picture archiving and communication system (PACS) workstation (DirectView, v. 11.3, Carestream Health) for tumor presentation, including quantitative and qualitative variables.

Several findings were evaluated by using a standardized data collection form. The following features of ACC of the pancreas were evaluated including largest transverse diameter of the tumor, tumor location (head, body, or tail), tumor shape (oval *vs.* round), tumor contours (well- *vs.* ill-defined) and presence of a tumor capsule (complete or incomplete). ACC were also classified as exclusively intrapancreatic when they were entirely surrounded by pancreatic parenchyma or with extrapancreatic growth when ACC had portions outside the pancreas. MRI examinations were also analyzed for the presence of Wirsung duct enlargement (diameter > 3 mm), bile duct dilatation, focal hepatic lesions, adjacent organ involvement, peritoneal nodule, free-fluid effusion, presence of lymph nodes, presence of

enlarged lymph nodes (> 10 mm), vascular encasement by tumor and segmental portal hypertension.

The internal signal intensity of ACC was defined by comparison with that of the apparently normal pancreatic parenchyma and was described as hypo-, iso-, or hyperintense on the different MRI sequences. Areas with signal intensity similar to that of the cerebrospinal fluid on both T1- and T2-weighted MR images were considered as cystic components of the tumor, whereas the others were considered solid. Finally, the contrast-enhancement patterns (marked, mild or absent; homogeneous or heterogeneous) of the tumor were also determined for all contrast-enhanced MR images. When a capsule was present, capsule enhancement was categorized as absent or present.

In addition, the observers measured mean apparent diffusion coefficient (ADC) values of pancreatic tumors using a manually drawn region of interest (ROI). A ROI as large as possible was drawn manually by each observer, excluding the edges of the tumor, to minimize the influence of the peripheral normal parenchyma on ADC measurement. ROIs were selected to have dimensions > 100 mm^2 or at least 100 pixels [9] when possible, depending on tumor size and placed on areas that did not contain pancreatic ducts, vessels or pancreatic fat. In addition, ROIs were placed to exclude cystic areas of ACC. The ADC value of each tumor was calculated using a mono-exponential fitting algorithm using the 3 b values (50, 400-500, and 800-1000 s/mm^2). ADC values were measured five times by each observer and the mean value of the ten measurements was tabulated for each ADC. Normalized ADC ratios were also calculated using the spleen as a reference organ [30-32] and defined as the ratio of pancreatic lesion ADC to splenic ADC.

MRI findings were compared to surgical and histopathological findings using the original surgical and histopathological reports and photographs of transversally sectioned gross specimens.

Statistical analysis

Statistical analysis was performed with Statview (SAS Institute,Cary, NC, USA). Quantitative data (continuous) were expressed as medians, first quartiles (q1), third quartiles (q3) and ranges. Qualitative data were expressed as raw numbers, proportions and percentages.

Results

The tumors were located in the head (n=2), body (n=2), and tail (n=1) of the pancreas. Median largest axial diameter of the tumors was 43 mm (Q_1, 35; Q_3, 82 mm; range: 30 – 91 mm).

All tumors were oval (5/5; 100%). On T1-weighted images, 3/5 tumors (60%) were hypointense (Fig. 1) and 2/5 were isointense (40%) (Fig. 2) relative to the adjacent pancreatic parenchyma. On T2-weighted MR images, 3/5 tumors (60%) tumors were isointense (Fig. 1) and 2/5 tumors (40%) were hyperintense (Fig. 3) relative to the adjacent pancreatic parenchyma. All tumors (5/5; 100%) showed mild and heterogeneous enhancement after intravenous administration of a gadolinium chelate on the different acquisition phases. Tumor capsule was observed in 4/5 tumors (80%), being complete in one tumor (Fig. 1) and incomplete in 3 tumors (Fig. 3).

On DW-MRI, all tumors (5/5; 100%) were hyperintense on the 3 b value images relative to the adjacent pancreatic parenchyma (Figs. 1-3). Median ADC value of ACC was 1.061×10^{-3} mm^2/sec (Q_1, 0.870×10^{-3} mm^2/sec; Q_3, 1.138×10^{-3} mm^2/sec; range: $0.834\text{-}1.195 \times 10^{-3}$ mm^2/sec). Median splenic ADC value was 0.971×10^{-3} mm^2/sec (Q_1, 0.734×10^{-3} mm^2/sec; Q_3, 1.000×10^{-3} mm^2/sec; range: $0.729\text{-}1.007 \times 10^{-3}$ mm^2/sec). Median normalized ADC ratio of ACC was 1.127 (Q_1, 1.071; Q_3, 1.237; range: 1.054-1.244) (Table 1).

Enlargement of the Wirsung duct distal to tumor was present in 2/5 patients (40%); these two patients had a tumor of the pancreatic head and the pancreatic tail (one each). Enlargement of the Wirsung duct was observed in association with pancreatic parenchyma atrophy in 1/5 patient (20%) (Fig. 2). No patient had bile duct dilatation present on MR images.

Vascular encasement was observed in 2/5 tumors (40%) and consisted in splenic vein encasement (Fig. 3) as confirmed by histopathological analysis. Involvement of adjacent organs were present in 2/5 patients (40%); consisting in duodenal involvement in one patient and splenic involvement in one patient. Hepatic metastases were visible in 2/5 patients (40%), being hypervascular in both. Enlarged lymph nodes adjacent to ACC were observed in 1/5 patient (20%) and confirmed at histopathological analysis (Fig. 3). Peritoneal nodules and peritoneal fluid effusion were observed in no patients.

Discussion

In the present study we report the MRI features of ACC of the pancreas in five patients. We found that on MRI, ACC of the pancreas predominantly presents as a large, oval, encapsulated, solid pancreatic mass with moderate and heterogeneous enhancement after intravenous administration of a gadolinium chelate. In addition, we found that all ACC of the pancreas are visible on DW-MRI with a median ADC value of 1.061 x 10^{-3} mm^2/sec and a median normalized ADC ratio of 1.127.

DW-MRI has been regarding as a promising tool for the characterization of pancreatic lesions [2, 5, 6]. In this regard, DW-MRI may help differentiate between pancreatic cancer and focal chronic pancreatitis and characterize the content of cystic tumors [33]. An analysis of the results of the literature found a mean ADC value of 1.332 x 10 -3 mm^2/sec for ductal ADC and 1.538 for neuroendocrine tumors of the pancreas [8]. However, to date no studies have reported the ADC values of ACC of the pancreas. In addition, in this study we have calculated the normalized ADC ratios of ACC tumors, which may provide a more robust reference for further comparison [8, 9, 30].

The wide imaging spectrum of ACC has been highlighted by previous reports [15, 17, 18, 25]. In this regard, Tatli et al. have reported the MRI findings in two patients with ACC of the pancreas [25]. One tumor was solid, hypointense on T1-weighted MR images, hyperintense on T2-weighted MR images relative to the apparently healthy pancreatic parenchyma. The other tumor was partially cystic and well marginated. The central portion had mixed signal intensity on T1-weighted MR images and was hyperintense on T2-weighted MR images [25]. In the same study, the tumor showed homogeneous enhancement but less marked than that of the pancreatic parenchyma [25]. Our results show that encapsulation and tumor enhancement may be suggestive features for the diagnosis of ACC although encapsulation has been reported as a frequent finding in other tumors such as solid and pseudopapillary tumors [34]. Matsumoto et al. reported one ACC tumor of the pancreas that resembled solid and papillary tumor of the pancreas in a 34-year-old woman [14]. In addition, in the same patient, histopathological analysis of tumor samples obtained from percutaneous biopsy was misleading so that the definite diagnosis was obtained after surgical resection [14]. DW-MRI may be of interest to differentiate between ACC of the pancreas and solid and pseudopapillary tumor. In our study, the median ADC value of ACC was 1.061 × 10^{-3} mm^2/sec with values ranging between 0.834 10^{-3} mm^2/sec and 1.195 × 10^{-3} mm^2/sec. On the opposite, solid and pseudopapillary tumors have a mean ADC value of 1.208 10^{-3} mm^2/sec with ADC values

ranging between 1.050 10^{-3} mm^2/sec and 2.793 10^{-3} mm^2/sec [8]. However, further studies assessing the capabilities of DW-MRI to discriminate between these two entities are needed.

In the present study, we have described in details the MRI features of 5 ACC. However, comparison with prior studies is sometimes difficult. In this regard, Matsumoto et al. have reported three ACC of the pancreas in three different patients [14]. However, the main goal of their study was not to describe the MRI features of ACC. As a consequence, they only briefly described the MRI features of the tumors as hypointense on T1-weighted images and hyperintense on T2-weighted images, similar to our study. In the same study, the dynamic features were described as “high contrast on the dynamic study” for one tumor and “slightly enhancing” for another one [14]. However, these researchers showed MR images of only one tumor in their paper [14]. In our patients, the five tumors showed mild enhancement that was less marked than that of the adjacent and apparently uninvolved pancreatic parenchyma. These results are consistent with those of Hsu et al. [28]. Several researchers have reported unusual imaging features of ACC of the pancreas that were not observed in our patients [14, 24]. It is thus acknowledged that ACC of the pancreas exhibits a wide range of presentation so that the diagnosis may be difficult with imaging alone [14, 24]. Luo et al. have reported two patients with ACC presenting as a diffuse enlargement of the pancreatic gland displaying a “sausage-like” shape [24]. In these two patients, the tumors were heterogeneous on CT and showed intense uptake of 18F-fluorodeoxyglucose on positron emission tomography/CT. However, the patients did not undergo MRI [24]. Hashimito et al. have reported similar “sausage-like” shape in one patient but the MR images were not displayed in the case presentation [23]. In our study, no patients had ACC with a “sausage-like” shape.

In our study, two patients had ACC of the pancreatic head that was responsible for Wirsung duct dilatation and upstream parenchymal atrophy of the pancreas. This finding has been reported by Kim et al. who have reported two histopathologically confirmed intraductal and papillary variants of ACC that mimicked intraductal papillary mucinous neoplasm of the pancreas [26]. In our patient with Wirsung duct dilatation the presentation was different as the ACC presented as an intrapancreatic mass with upstream Wirsung duct dilatation. In our study, no patients had bile duct dilatation even those with ACC tumor located in the pancreatic head. This absence of bile duct dilatation in patients with ACC may be explained by the origin of the ACC. ACC indeed originates from acinar cell of the pancreas and not from the ductal epithelium [23]. Hu et al. found bile duct dilatation in only1/10 patients with ACC of the pancreas, thus confirming that this finding is rare in ACC, contrary to in the more

common pancreatic adenocarcinoma [21]. Nagata et al. reported that obstructive jaundice in patient with ACC can be due to intrahepatic bile duct metastases of ACC of the pancreatic head and not to compression [35].

Our study has some limitations. Of these, the small number of patients may be a limitation to cover the entire spectrum of MR imaging presentation of ACC of the pancreas. This small number is also a limitation to make a comparative study with other types of pancreatic tumors and identify MR imaging features that may be suggestive of ACC.

In conclusion, our study reveals that on MRI, ACC of the pancreas predominantly presents as an oval pancreatic mass with moderate and heterogeneous enhancement after intravenous administration of a gadolinium chelate, tumor capsule and a median ADC value of 1.061×10^{-3} mm^2/sec. Further studies however are needed to confirm our findings obtained in a limited number of patients.

Conflict of interest

The authors have no conflicts of interest to disclose regarding this article.

References

1. Frampas E, David A, Regenet N, Touchefeu Y, Meyer J, Morla O. Pancreatic carcinoma: key-points from diagnosis to treatment. Diagn Interv Imaging 2016;97:1207-23.
2. Barral M, Faraoun SA, Fishman EK, Dohan A, Pozzessere C, Berthelin MA, et al. Imaging features of rare pancreatic tumors. Diagn Interv Imaging 2016;97:1259-73.
3. Dromain C, Déandréis D, Scoazec JY, Goere D, Ducreux M, Baudin E, et al. Imaging of neuroendocrine tumors of the pancreas. Diagn Interv Imaging 2016;97:1241-57.
4. Chu LC, Singhi AD, Haroun RR, Hruban RH, Fishman EK. The many faces of pancreatic serous cystadenoma: radiologic and pathologic correlation. Diagn Interv Imaging 2017;98:191-202.
5. Hammond NA, Miller FH, Day K, Nikolaidis P. Imaging features of the less common pancreatic masses. Abdom Imaging 2013;38:561–572.
6. Shah S, Mortele K. Uncommon solid pancreatic neoplasms: ultrasound, computed tomography, and magnetic resonance imaging features. Semin Ultrasound CT MR 2007;28:357–70.
7. Bezerra ROF, Machado MC, Dos Santos Mota MM, Ezzedine TA, Siqueira LTB, Cerri GG. Rare pancreatic masses: a pictorial review of radiological concepts. Clin Imaging 2018;50:314-23.
8. Barral M, Taouli B, Guiu B, Koh DM, Luciani A, Manfredi R, et al. Diffusion-weighted MR imaging of the pancreas: current status and recommendations. Radiology 2015;274:45-63.
9. Barral M, Sebbag-Sfez D, Hoeffel C, Chaput U, Dohan A, Eveno C, Boudiaf M, Soyer P. Characterization of focal pancreatic lesions using normalized apparent diffusion coefficient at 1.5-Tesla: preliminary experience. Diagn Interv Imaging 2013;94:619-27.
10. Yeh R, Steinman J, Luk L, Kluger MD, Hecht EM. Imaging of pancreatic cancer: what the surgeon wants to know. Clin Imaging 2017;42:203-17.
11. Lotfalizadeh E, Ronot M, Wagner M, Cros J, Couvelard A, Vullierme MP, et al. Prediction of pancreatic neuroendocrine tumour grade with MR imaging features: added value of diffusion-weighted imaging. Eur Radiol 2017;27:1748-59.
12. Holen KD, Klimstra DS, Hummer A, Gonen M, Conlon K, Brennan M, Saltz LB. Clinical characteristics and outcomes from an institutional series of acinar cell carcinoma of the pancreas and related tumors. J Clin Oncol 2002;20:4673-8.

13. Matos JM, Schmidt CM, Turrini O, Agaram NP, Niedergethmann M, Saeger HD, et al. Pancreatic acinar cell carcinoma: a multi-institutional study. J Gastrointest Surg 2009;13:1495-502

14. Matsumoto S, Sata N, Koizumi M, Lefor A, Yasuda Y. Imaging and pathological characteristics of small acinar cell carcinomas of the pancreas: a report of 3 cases. Pancreatology 2013;13:320-3

15. Bhosale P, Balachandran A, Wang H, Wei W, Hwang RF, Fleming JB, et al. CT imaging features of acinar cell carcinoma and its hepatic metastases. Abdom Imaging 2013;38:1383-90.

16. Ong MJ, Tang YL, Tan CH. Clinics in diagnostic imaging (157). Acinar cell carcinoma (ACC) of the pancreatic tail. Singapore Med J 2014;55:564-7.

17. Liu K, Peng W, Zhou Z. The CT findings of pancreatic acinar cell carcinoma in five cases. Clin Imaging 2013;37:302-7.

18. Chiou YY, Chiang JH, Hwang JI, Yen CH, Tsay SH, Chang CY. Acinar cell carcinoma of the pancreas: clinical and computed tomography manifestations. J Comput Assist Tomogr 2004;28:180-6.

19. Raman SP, Hruban RH, Cameron JL, Wolfgang CL, Kawamoto S, Fishman EK. Acinar cell carcinoma of the pancreas: computed tomography features--a study of 15 patients. Abdom Imaging 2013;38:137-43.

20. Mustert BR, Stafford-Johnson DB, Francis IR. Appearance of acinar cell carcinoma of the pancreas on dual-phase CT. AJR Am J Roentgenol 1998;171:1709.

21. Hu S, Hu S, Wang M, Wu Z, Miao F. Clinical and CT imaging features of pancreatic acinar cell carcinoma. Radiol Med 2013;118:723-31.

22. Yang TM, Han SC, Wu CJ, Mo LR. Acinar cell carcinomas with exophytic growth and intraductal pancreatic duct invasion: peculiar multislice computed tomographic picture. J Hepatobiliary Pancreat Surg 2009;16:238-41.

23. Hashimoto M, Matsuda M, Watanabe G, Mori M, Motoi N, Nagai K, et al. Acinar cell carcinoma of the pancreas with intraductal growth: report of a case. Pancreas 2003;26:306–8.

24. Luo Y, Hu G, Ma Y, Guo N, Li F. Acinar cell carcinoma of the pancreas presenting as diffuse pancreatic enlargement: two case reports and literature review. Medicine 2017;96:e7904.

25. Tatli S, Mortele KJ, Levy AD, Glickman JN, Ros PR, Banks PA, et al. CT and MRI features of pure acinar cell carcinoma of the pancreas in adults. AJR Am J Roentgenol 2005;184:511-9.

26. Kim HJ, Kim YK, Jang KT, Lim JH. Intraductal growing acinar cell carcinoma of the pancreas. Abdom Imaging 2013;38:1115-9.
27. Mergo PJ, Helmberger TK, Buetow PC, Helmberger RC, Ros PR. Pancreatic neoplasms: MR imaging and pathologic correlation. Radiographics 1997;17:281-301.
28. Hsu MY, Pan KT, Chu SY, Hung CF, Wu RC, Tseng JH. CT and MRI features of acinar cell carcinoma of the pancreas with pathological correlations. Clin Radiol 2010;65:223-9.
29. Soyer P, Dohan A, Patkar D, Gottschalk A. Observational study on the safety profile of gadoterate meglumine in 35,499 patients: The SECURE study. J Magn Reson Imaging 2017;45:988-97.
30. Soyer P, Kanematsu M, Taouli B, Koh DM, Manfredi R, Vilgrain V, et al. ADC normalization: a promising research track for diffusion-weighted MR imaging of the abdomen. Diagn Interv Imaging 2013;94:571-3.
31. Do RKG, Chandanara H, Felker E, Hajdu CH, Babb JS, Kim D, et al. Diagnosis of liver fibrosis and cirrhosis with diffusion-weighted imaging: value of normalized apparent diffusion coefficient using the spleen as reference organ. AJR Am J Roentgenol 2010;195:671-6.
32. Papanikolaou N, Gourtsoyianni S, Yarmenitis S, Maris T, Gourtsoyiannis N. Comparison between two-point and four-point methods for quantification of apparent diffusion coefficient of normal liver parenchyma and focal lesions: value of normalization with spleen. Eur J Radiol 2010;73:305-9.
33. Pozzessere C, Castaños Gutiérrez SL, Corona-Villalobos CP, Righi L, Xu C, Lennon AM, et al. Diffusion-weighted magnetic resonance imaging in distinguishing between mucin-producing and serous pancreatic cysts. J Comput Assist Tomogr 2016;40:505-12.
34. Guerrache Y, Soyer P, Dohan A, Faraoun SA, Laurent V, Tasu JP, et al. Solid-pseudopapillary tumor of the pancreas: MR imaging findings in 21 patients. Clin Imaging 2014;38:475-82.
35. Nagata S, Tomoeda M, Kubo C, Yoshizawa H, Yuki M, Kitamura M, et al. Intraductal polypoid growth variant of pancreatic acinar cell carcinoma metastasizing to the intrahepatic bile duct 6 years after surgery: a case report and literature review. Pancreatology 2012;12:23-6.

Legends for figures

Figure 1. Magnetic resonance imaging (MRI) examination in an 86-year-old man with acinar cell carcinoma (ACC) of the pancreatic head. **A**, Fat-saturated T1-weighted MR image of the abdomen in the transverse plane shows large tumor (arrow) of the pancreatic head that is hypointense relative to the pancreatic parenchyma. **B**, Fat-saturated T1-weighted MR image of the abdomen in the transverse plane at a upper level than in **A** reveals that the pancreas shows normal appearance with no dilatation of the Wirsung duct. **C**, T2-weighted MR image in the transverse plane shows that the tumor (arrow) is isointense relative to the pancreatic parenchyma. **D**, T1-weighted MR image of the abdomen in the transverse plane obtained after intravenous administration of a gadolinium chelate during the portal venous phase shows heterogeneous and mild enhancement and complete tumor encapsulation (arrow). **E, F**, Diffusion-weighted MR images of the abdomen in the transverse plane obtained vith b values of 50 s/mm^2 (E), and 1000 s/mm^2 (F) show hyperintense tumor (arrows) indicating restricted diffusion. The tumor has an apparent diffusion coefficient of 0.834×10^{-3} mm^2/s. **G**, T1-weighted MR image of the abdomen in the transverse plane obtained after intravenous administration of a gadolinium chelate shows duodenal involvement (arrow) by tumor. **H**, Photograph shows gross appearance of ACC after surgical resection. Arrow indicates tumor capsule. Arrowhead shows duodenal involvement.

Figure 2. Magnetic resonance imaging (MRI) examination in a 61-year-old man with acinar cell carcinoma (ACC) of the pancreatic head. **A**, Fat-saturated T1-weighted MR image of the abdomen in the transverse plane shows tumor (arrow) of the pancreatic head. **B**, T2-weighted MR image of the abdomen in the transverse plane shows that the tumor (arrow) is hyperintense relative to the pancreatic parenchyma. The tumor is responsible for enlargement of the Wirsung duct (arrowhead). **C**, Diffusion-weighted MR images of the abdomen in the transverse plane obtained with b value of 1000 s/mm^2 show hyperintense tumor (arrow) indicating restricted diffusion. The tumor has an apparent diffusion coefficient of 1.061×10^{-3} mm^2/s. **D**, T1-weighted MR image of the abdomen in the transverse plane obtained during the arterial phase after intravenous administration of a gadolinium chelate shows hypervascular hepatic metastasis (arrow).

Figure 3. Magnetic resonance imaging (MRI) examination in a 68-year-old woman with acinar cell carcinoma (ACC) of the pancreatic tail. **A**, T2-weighted MR image of the abdomen in the transverse plane shows that pancreatic tumor (arrow) that is hyperintense relative to the pancreatic parenchyma. **B**, T1-weighted MR image of the abdomen in the transverse plane obtained during the portal venous phase after intravenous administration of a gadolinium chelate shows heterogeneous, incompletely encapsulated tumor (arrow) and splenic involvement. **C**, Diffusion-weighted MR images of the abdomen in the transverse plane obtained with b value of 1000 s/mm^2 show hyperintense tumor (arrow) indicating restricted diffusion. The tumor has an apparent diffusion coefficient of 1.081×10^{-3} mm^2/s. Enlarged lymph nodes are present. **D**, Photograph shows gross appearance of ACC after surgical resection. Arrow indicates splenic vein involvement. Arrowhead indicates metastatic lymph node.

Table 1. Demographic and MR imaging findings in 5 patients with pancreatic acinar cell carcinoma.

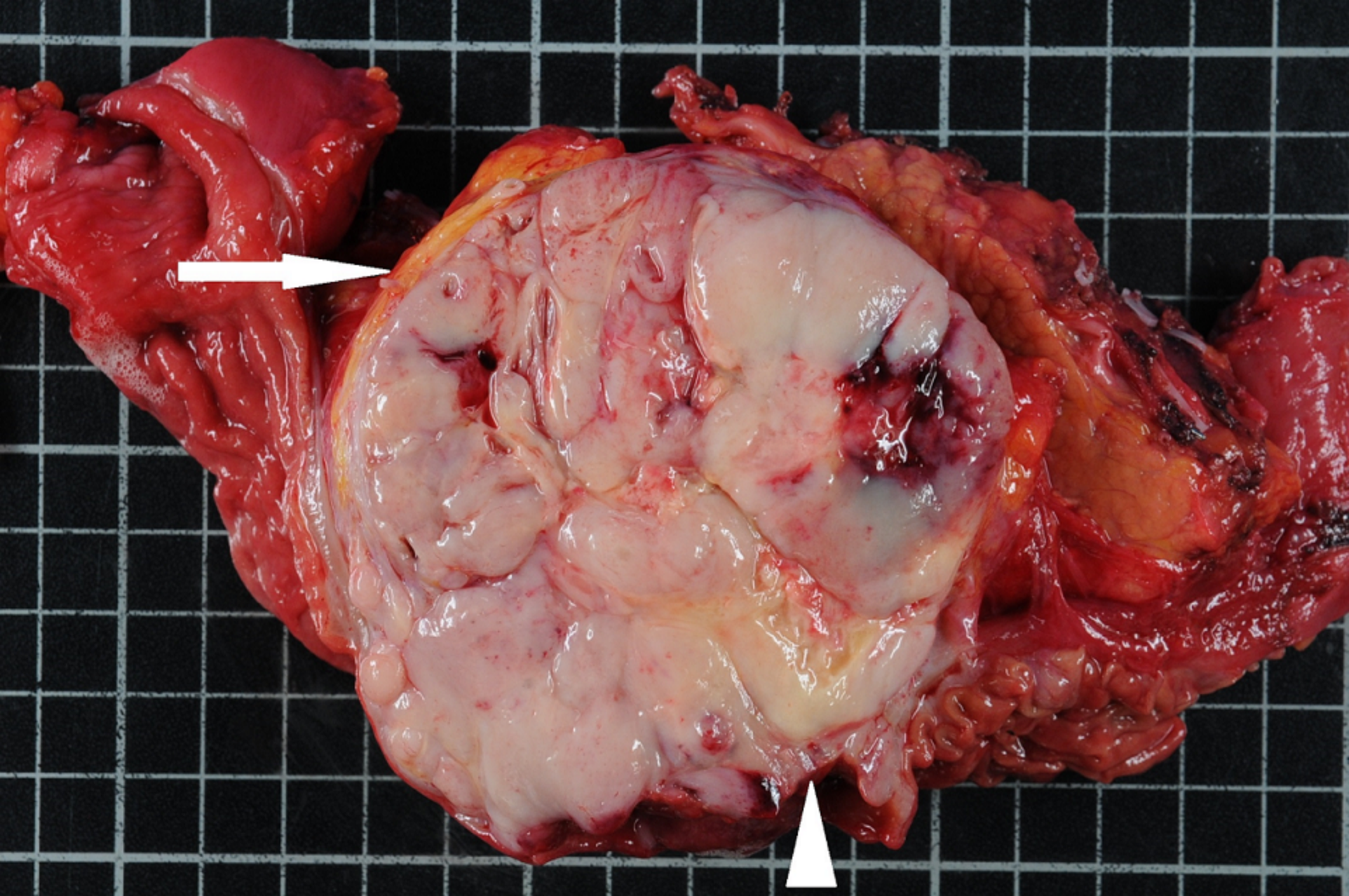

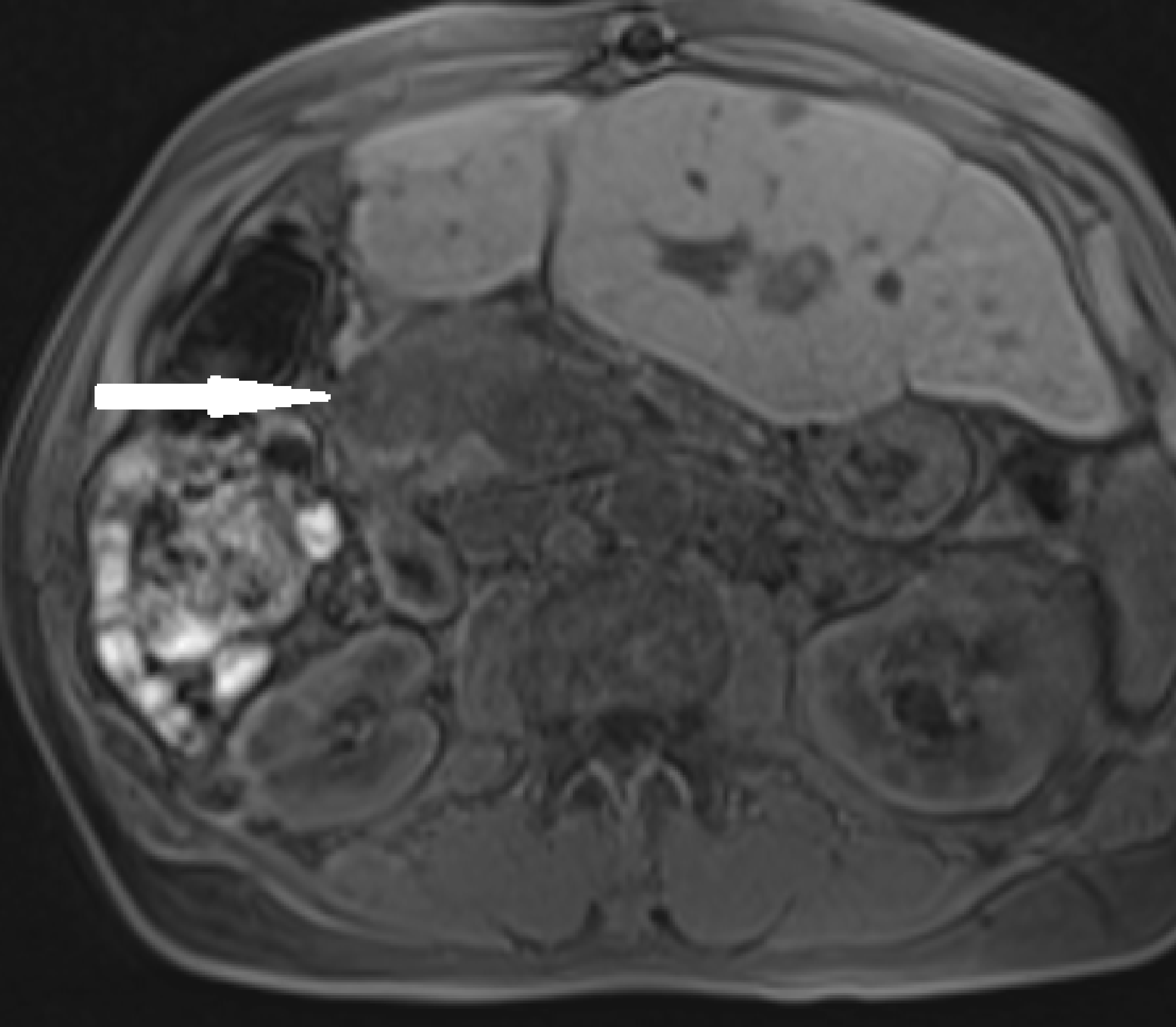

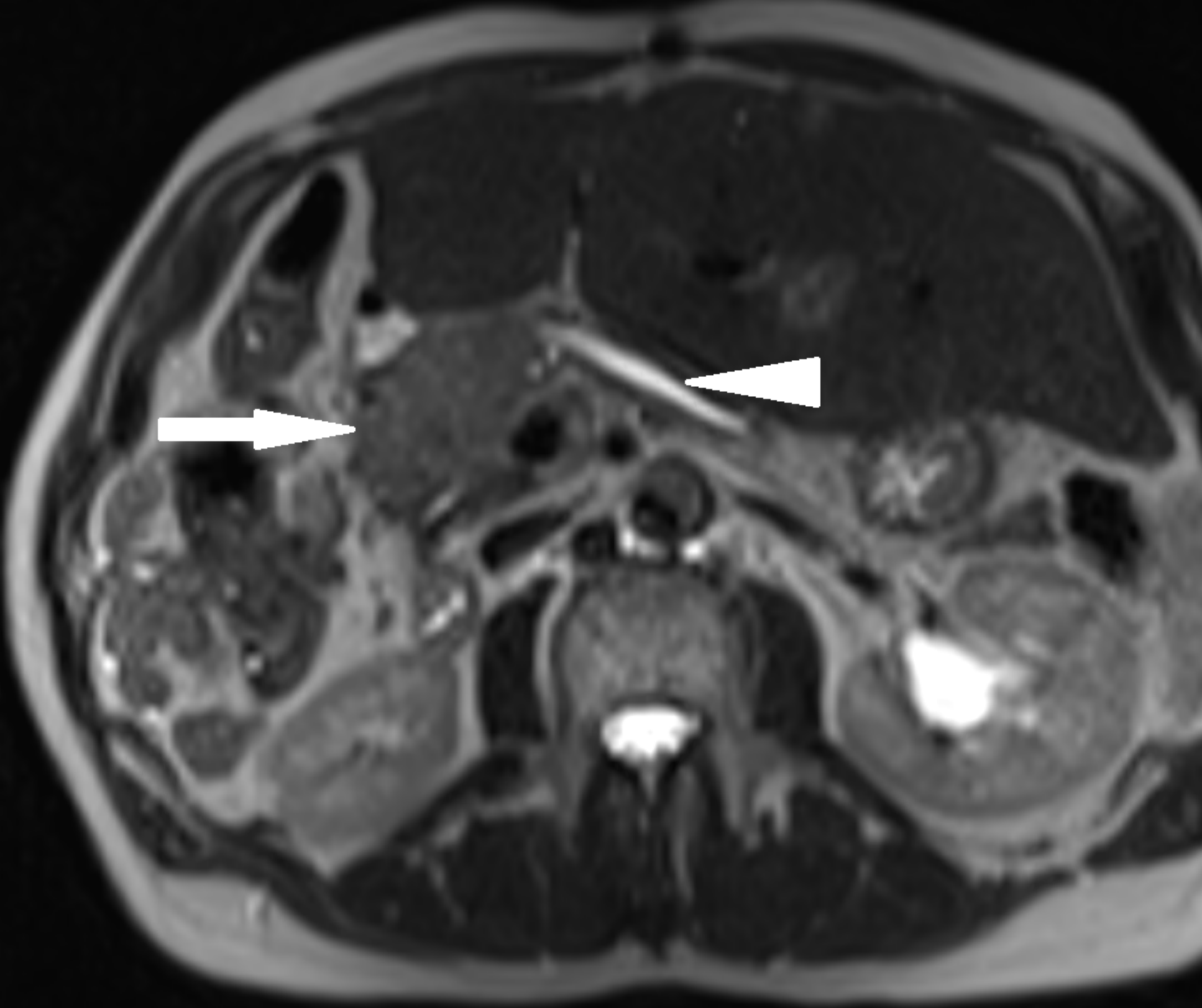

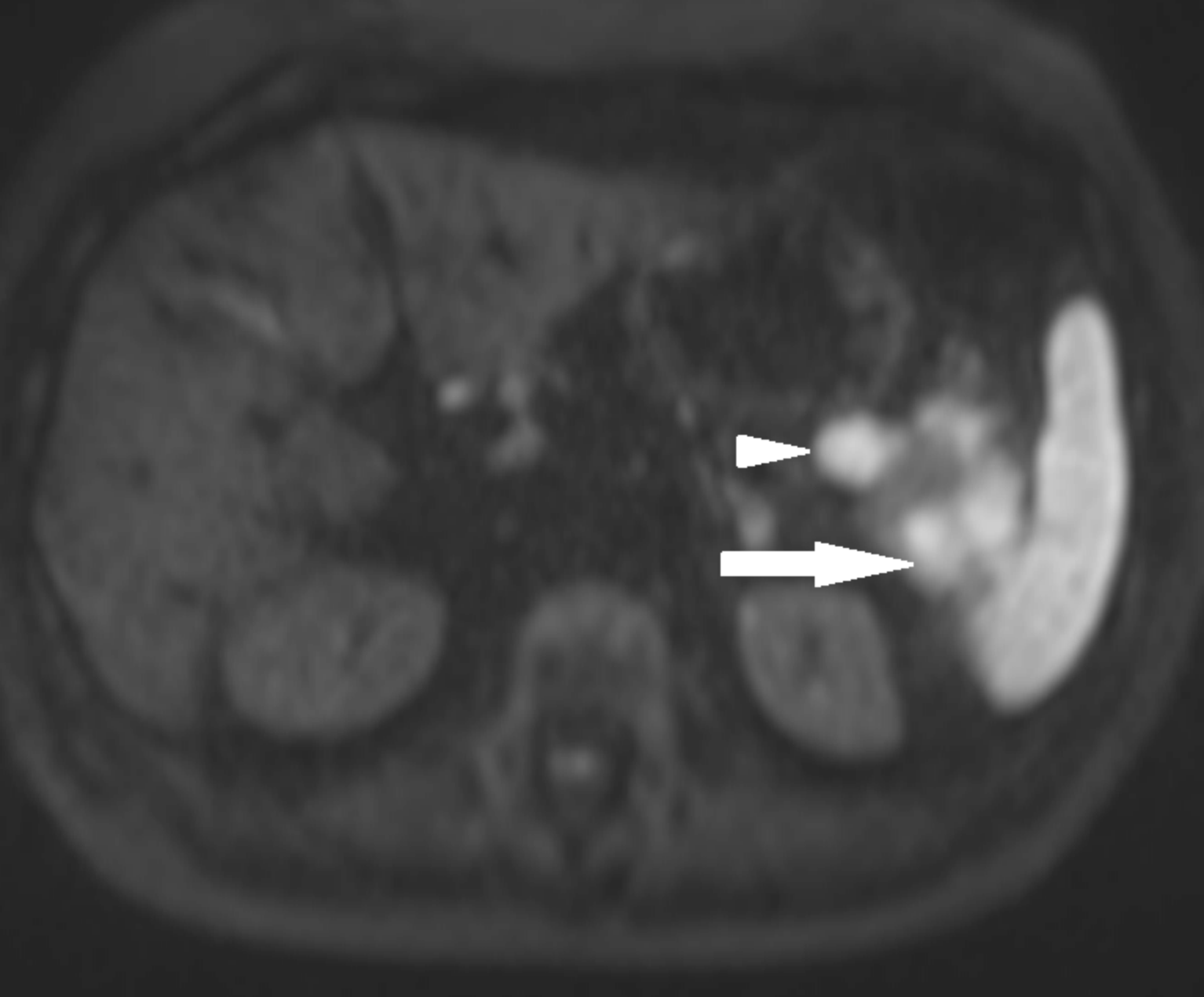

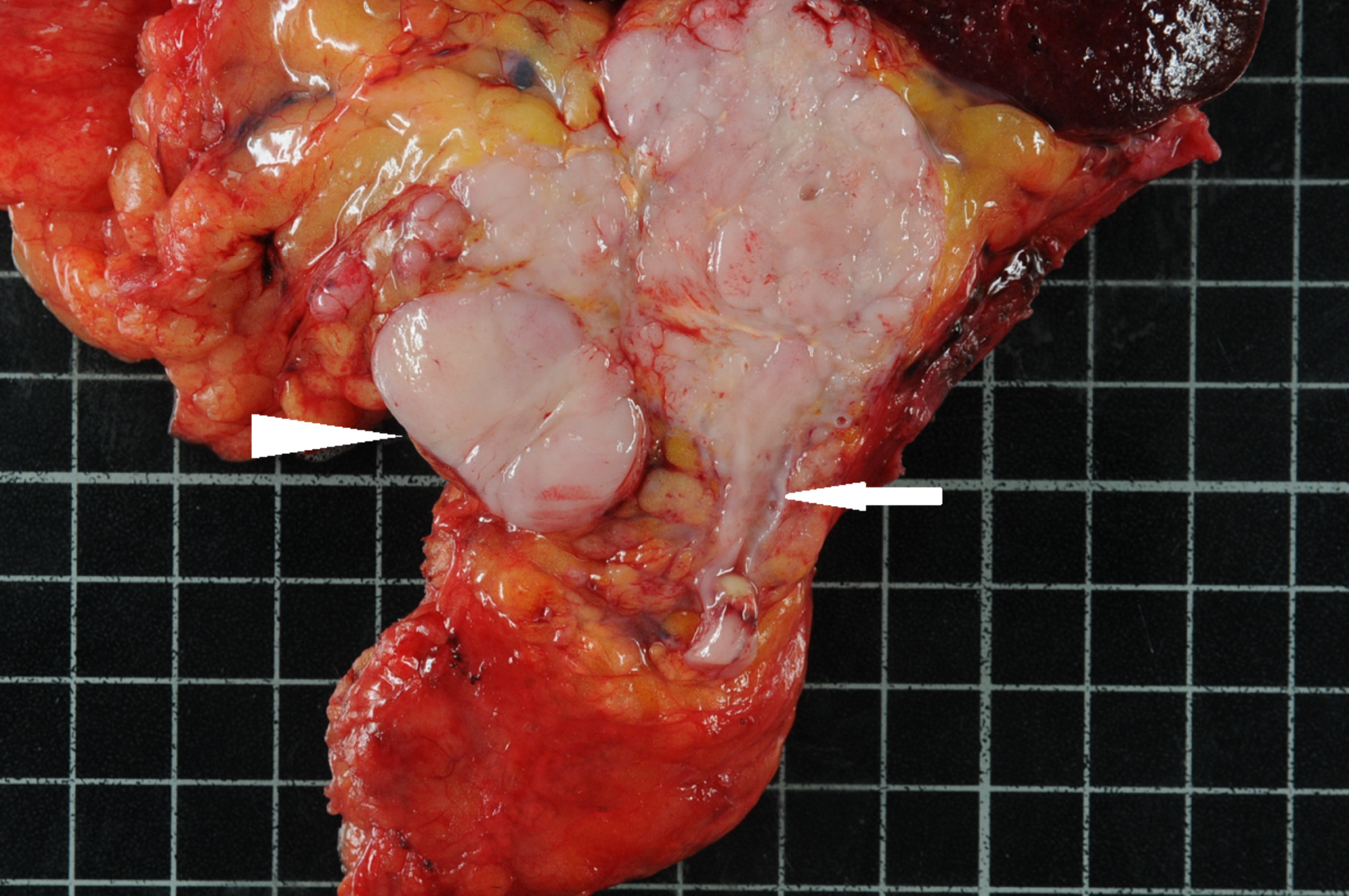

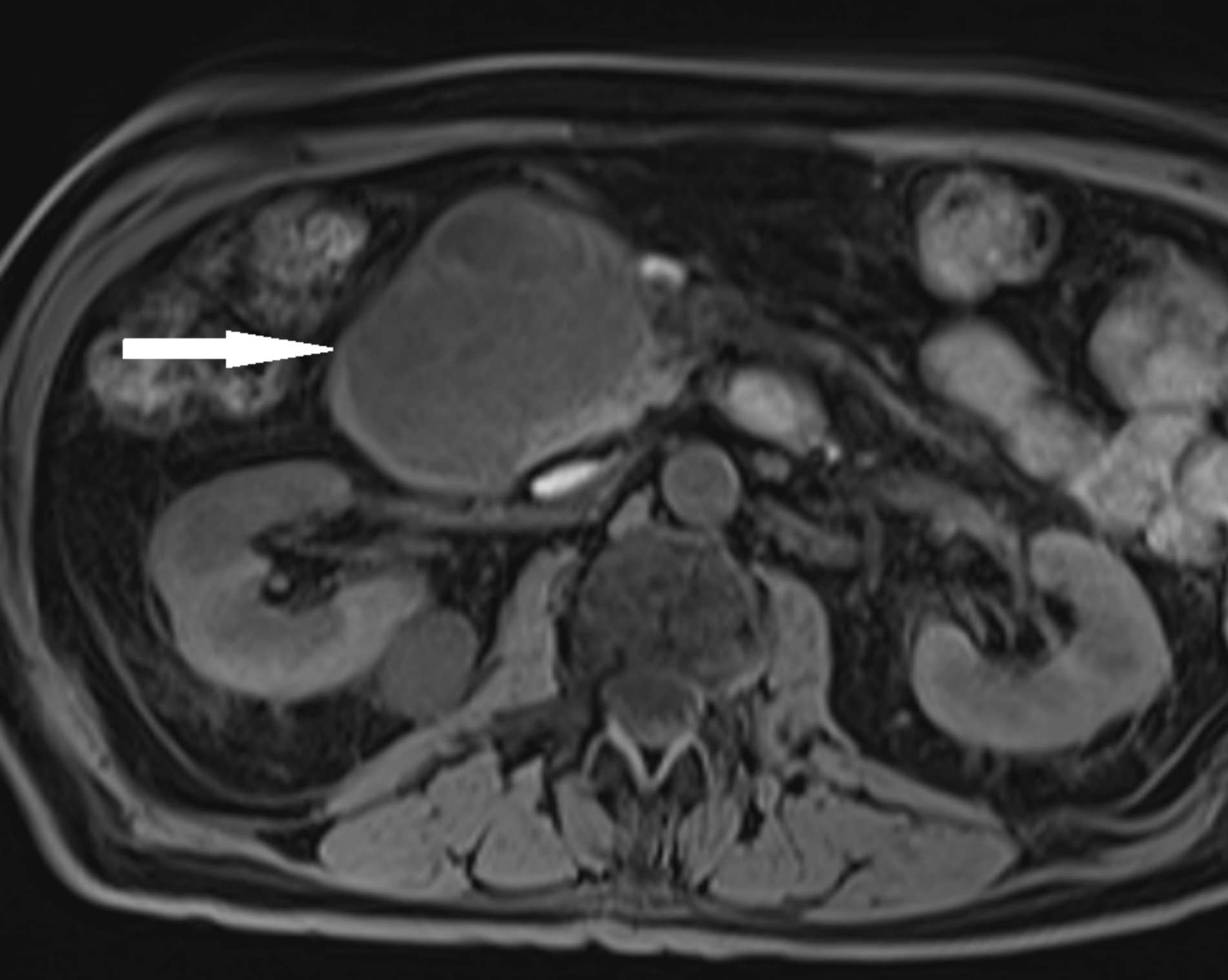

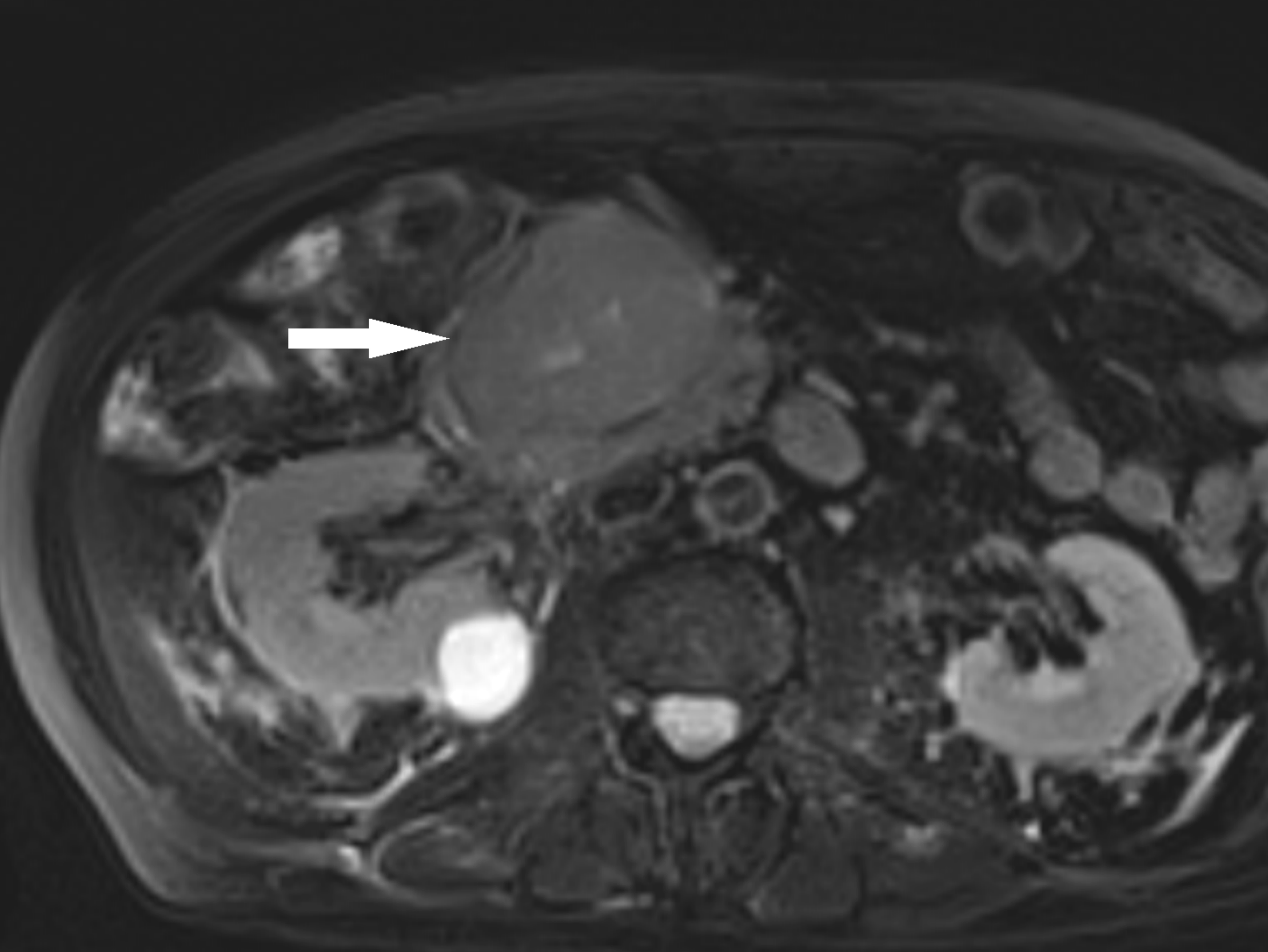

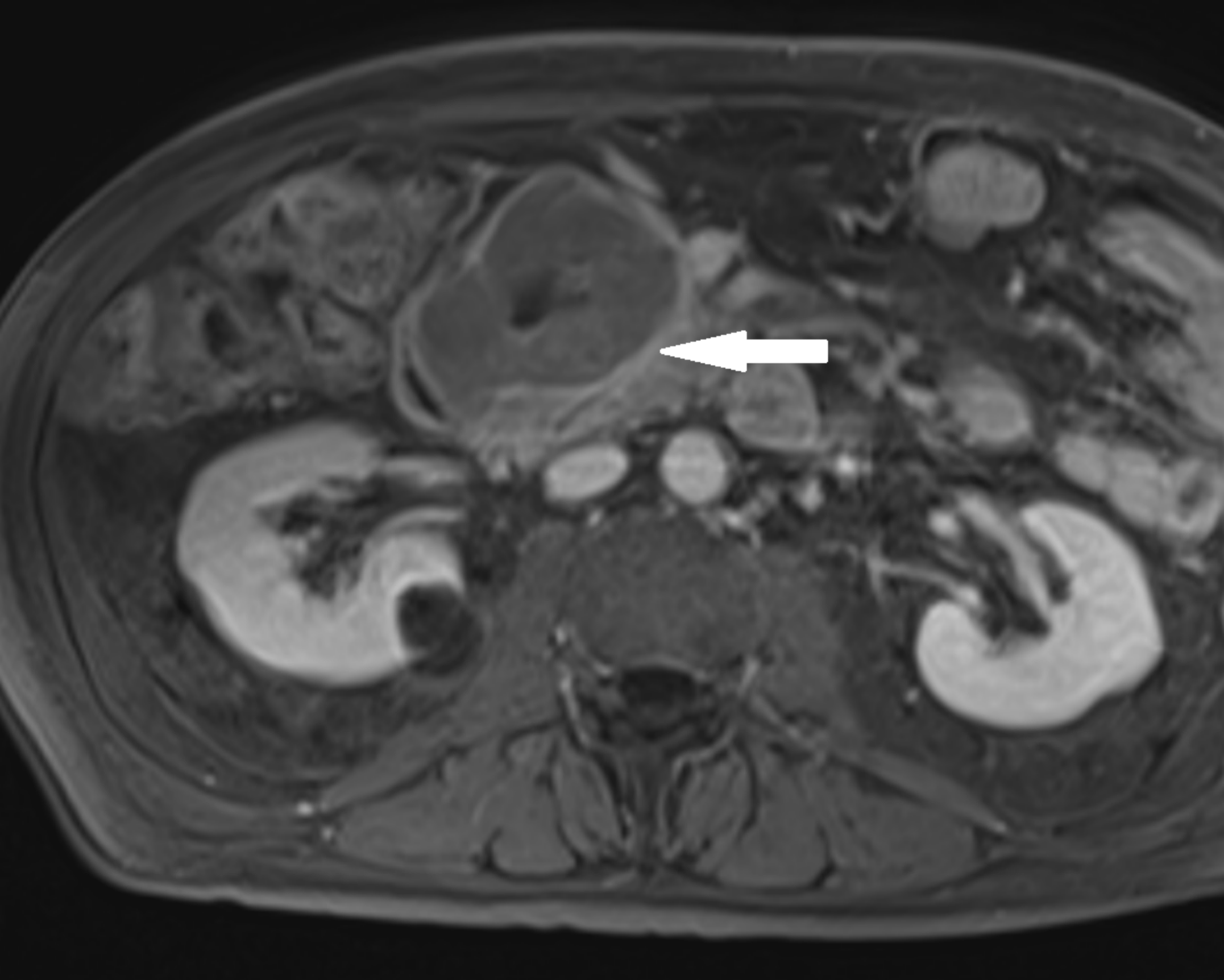

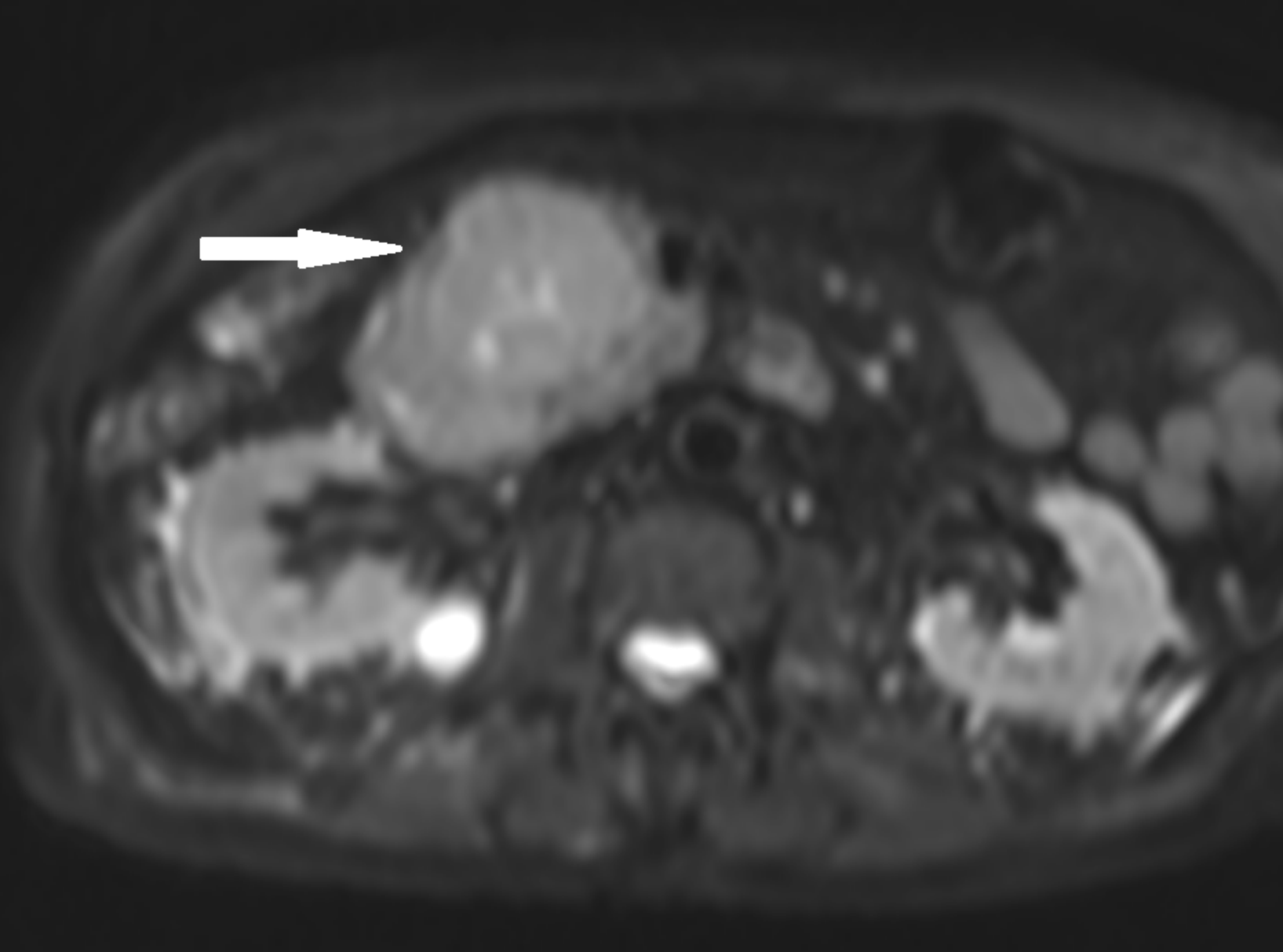

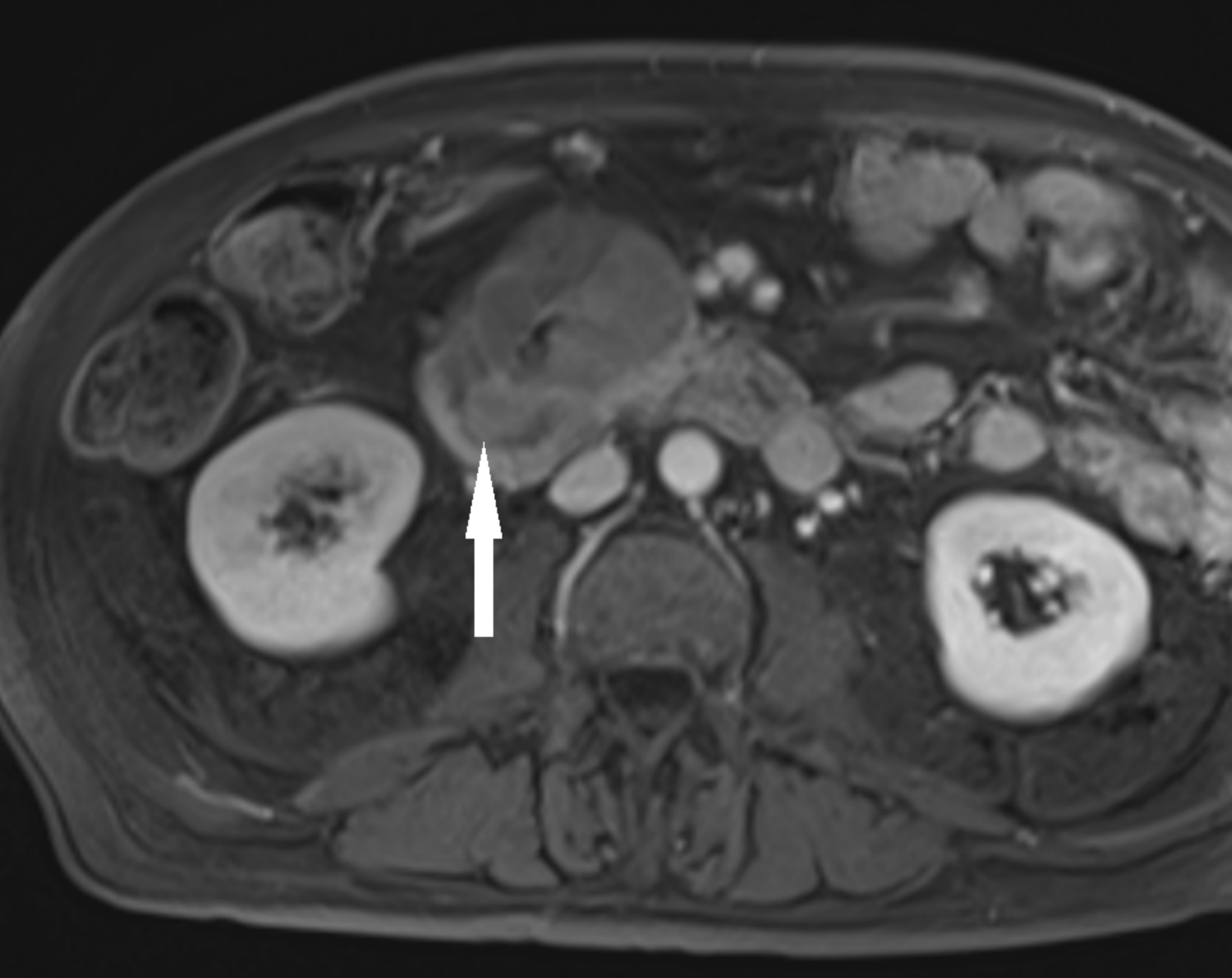

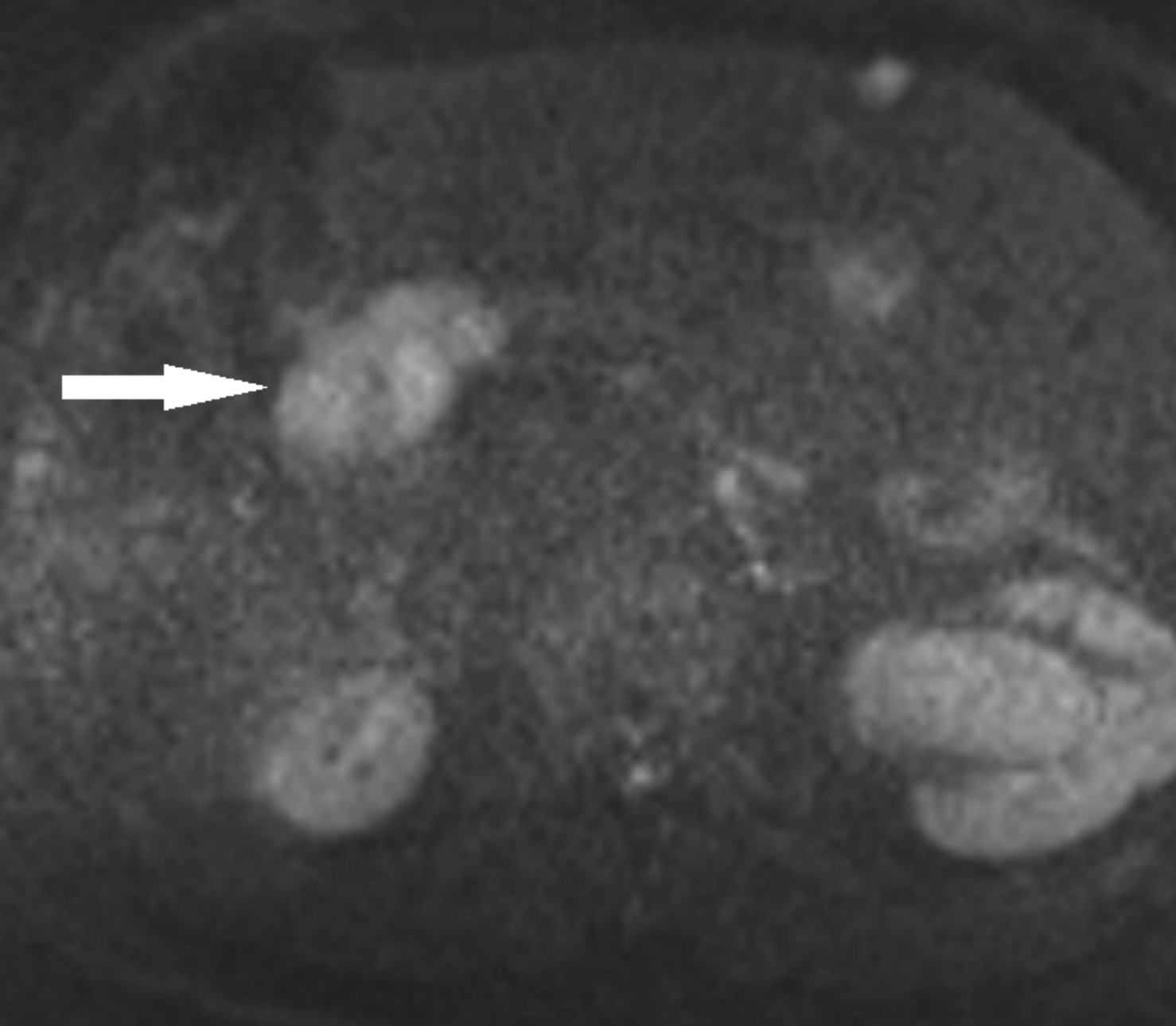

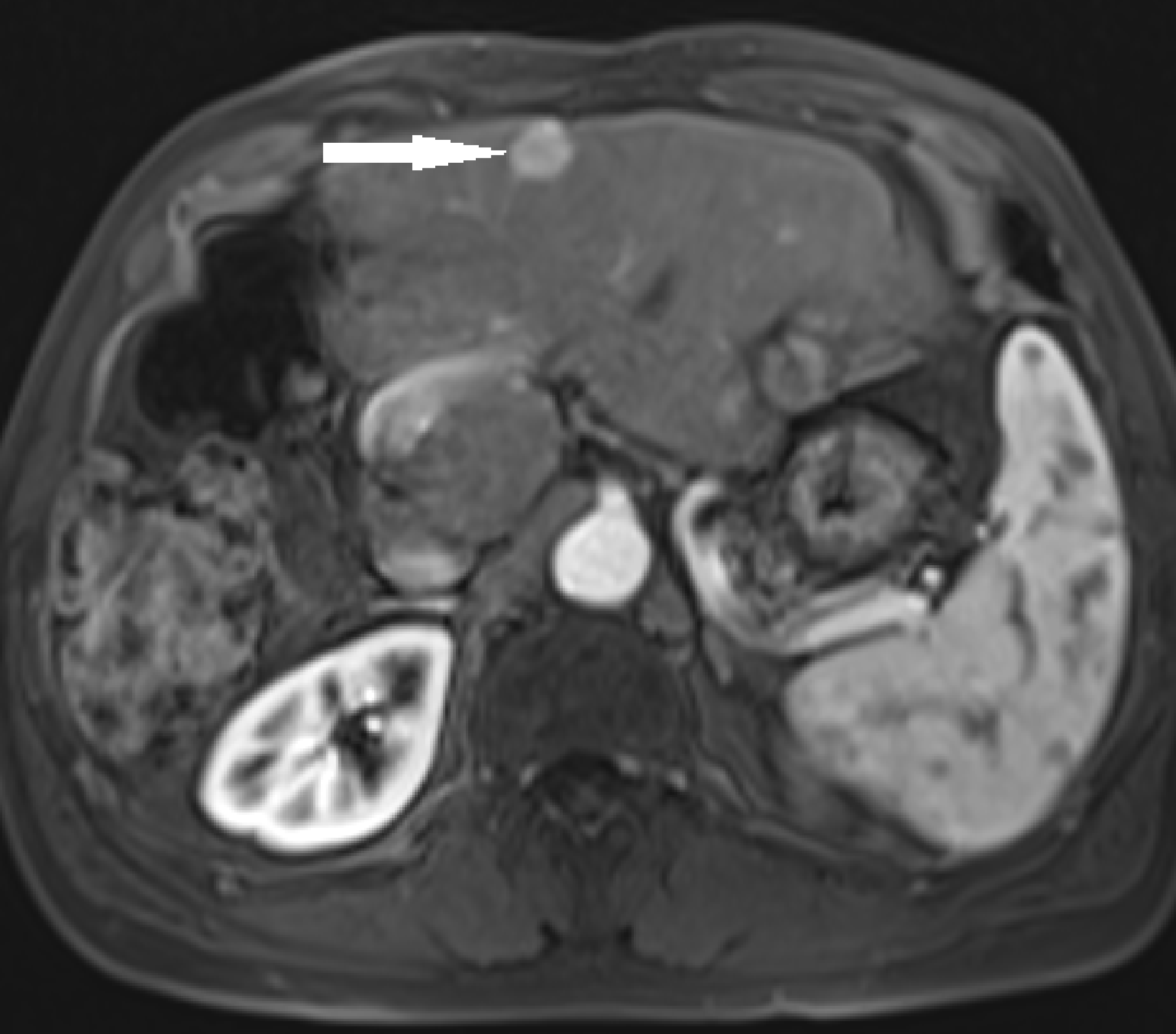

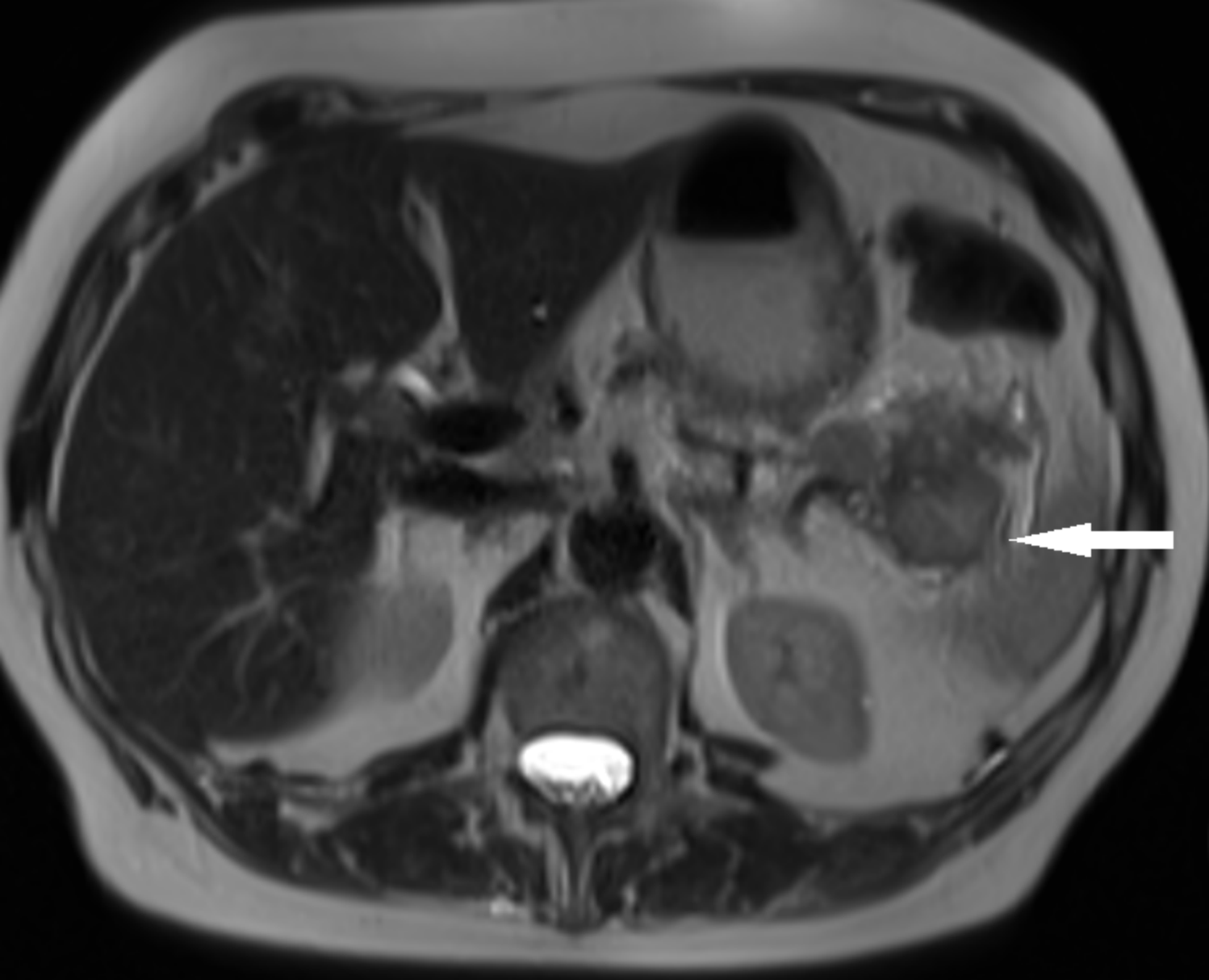

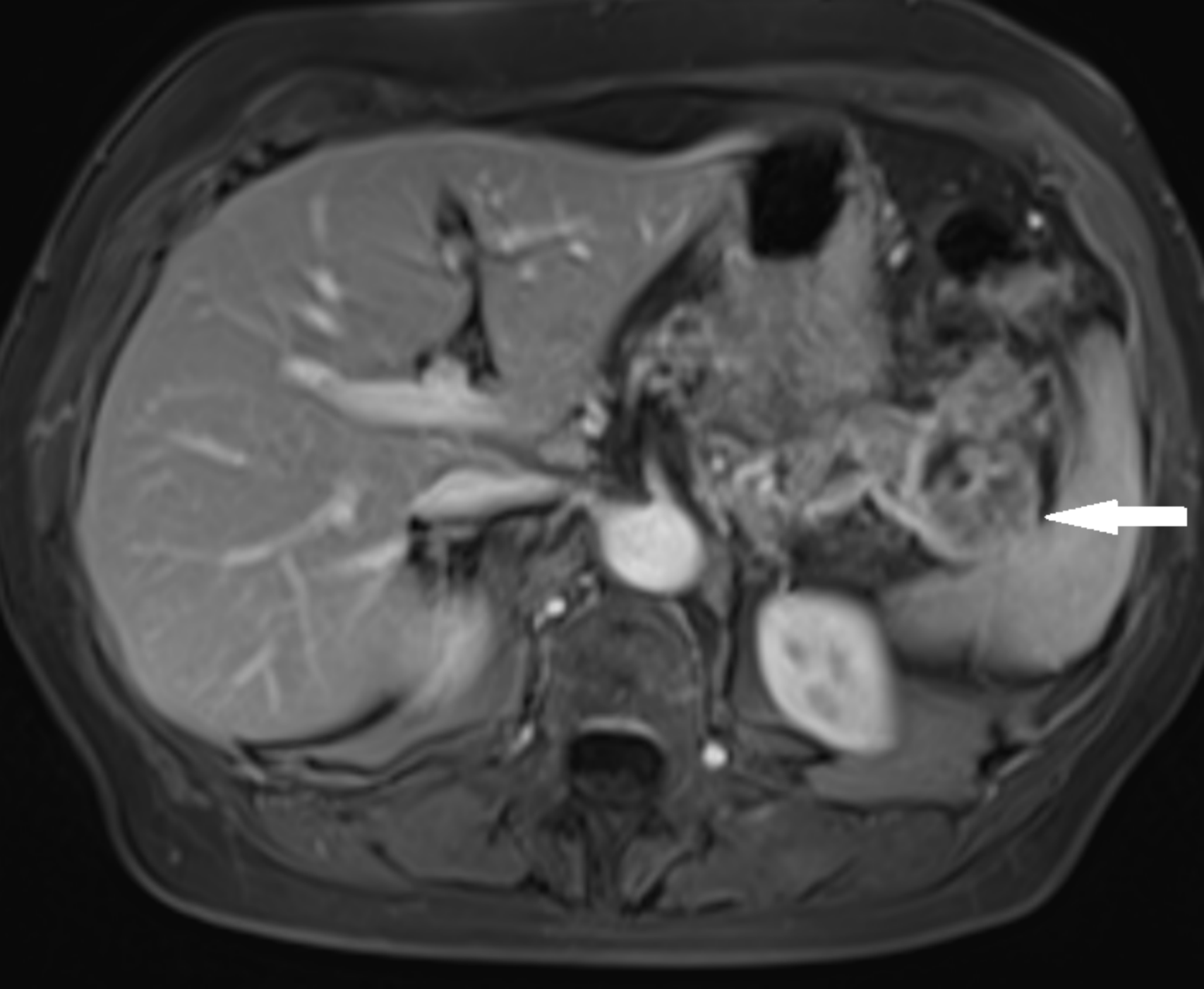

	Patient 1	Patient 2	Patient 3	Patient 4	Patient 5
Age (year)/Gender	61/M	86/M	68/F	38/F	61/M
Tumor location	Body	Head	Tail	Body	Head
Tumor shape	Oval	Oval	Oval	Oval	Oval
Largest diameter (mm)	30	73	43	91	41
Tumor contours	Ill defined	Well defined	Well defined	Well defined	Well defined
Capsule	No	Thin Complete Enhancing	Thin Incomplete Enhancing	Thin Incomplete Enhancing	Thin Incomplete Enhancing
Exophytic growth	No	Yes	Yes	Yes	No
Cystic portion	No	Yes	No	Yes	No
T1 signal intensity	Isointense	Hypointense	Hypointense	Hypointense	Isointense
T2 signal intensity	Isointense	Isointense	Hyperintense	Isointense	Hyperintense
Signal intensity on DWI	Hyperintense	Hyperintense	Hyperintense	Hyperintense	Hyperintense
Tumor ADC (x 10^{-3} mm^2/s)	1.195±0.092	0.834± 0.119	1.081±0.100	0.907±0.128	1.061±0.174
Spleen ADC (x 10^{-3} mm^2/s)	0.971±0.091	0.740±0.039	0.993±0.054	0.729±0.058	1.007±0.103
Normalized ADC	1.231	1.127	1.089	1.244	1.054
Tumor enhancement	Moderate and heterogeneous	Moderate and heterogeneous	Moderate and heterogeneous	Moderate and heterogeneous	Moderate and heterogeneous
Necrosis	No	Yes	Yes	Yes	No
Hemorrhage	No	No	No	Yes	No
Wirsung duct > 3 mm	Yes	No	No	No	Yes
Vascular involvement	Yes	No	Yes	No	No
Segmental portal hypertension	Yes	No	Yes	No	No
Hepatic metastases	Yes	No	No	No	Yes
Bile duct dilatation	No	No	No	No	No
Adjacent organ involvement	No	Duodenum	Spleen	No	No

Note. M = male; F = female; ADC = apparent diffusion coefficient; DWI = diffusion-weighted MR imaging.